

PROGRESS REPORT: PRESSURE VESSEL BURST TEST STUDY

Maurice R. Cain, Robert J. Hail
GPS Technologies, Inc.
Titusville, Florida

ABSTRACT

A progress report is provided on a program developed to study through test and analysis, the characteristics of blast waves and fragmentation generated by ruptured gas filled pressure vessels. Prior papers^{1, 2, 3, and 4} on this USAF/NASA program have been presented to AIAA, to JANNAF, to the NASA Pressure Systems Seminar and to a DOD Explosives Safety Board subcommittee meeting.

One Vessel has been burst with water pressure and eighteen with pneumatic pressure. All of the planned testing has been completed with the last test series having been completed in November 1993. The tests were designed to have a predetermined burst geometry and pressure level to study burst characteristics in an instrumented arena. Data trends for experiments are presented.

The paper presents results from the last test series which were not available earlier and compares all the pneumatic burst test results.

I. INTRODUCTION

Pressure vessels are used extensively in both ground and spacecraft applications. Explosive failures of vessels are rare due to precautions normally taken including adherence to consensus design, fabrication and test codes and standards. In service integrity is maintained through monitoring of vessel service conditions and cyclic history. Yet pressure vessels do occasionally fail, releasing significant energy and possible hazardous commodities into the surroundings. Often it is prudent to assess the damage that could result from explosive failure when locating pressure vessels, designing nearby structures and equipment, performing pressure tests, or considering other safety precautions.

A considerable body of data exists on damage and injury due to blast wave and fragmentation, much of it from research using TNT or similar high explosives. However substantially less is known about blast and fragmentation of bursting pressure vessels than of chemical explosions such as TNT. Further, current methods documented in standards, handbooks and other references used to quantify expected energy release, blast waves, and fragmentation are inconsistent and vary in result Accordingly, a pressure vessel burst test program has been conducted for the

—————*Reprinted from ASME Publication PVP Vol. 277, ASME Conference, 1994.

*This work was performed under FO865093C0066 with the 45th Space Wing, PAFB, Florida.

Report Documentation Page

*Form Approved
OMB No. 0704-0188*

Public reporting burden for the collection of information is estimated to average 1 hour per response, including the time for reviewing instructions, searching existing data sources, gathering and maintaining the data needed, and completing and reviewing the collection of information. Send comments regarding this burden estimate or any other aspect of this collection of information, including suggestions for reducing this burden, to Washington Headquarters Services, Directorate for Information Operations and Reports, 1215 Jefferson Davis Highway, Suite 1204, Arlington VA 22202-4302. Respondents should be aware that notwithstanding any other provision of law, no person shall be subject to a penalty for failing to comply with a collection of information if it does not display a currently valid OMB control number.

1. REPORT DATE AUG 1994	2. REPORT TYPE	3. DATES COVERED 00-00-1994 to 00-00-1994			
4. TITLE AND SUBTITLE Progress Report: Pressure Vessel Burst Test Study		5a. CONTRACT NUMBER			
		5b. GRANT NUMBER			
		5c. PROGRAM ELEMENT NUMBER			
6. AUTHOR(S)		5d. PROJECT NUMBER			
		5e. TASK NUMBER			
		5f. WORK UNIT NUMBER			
7. PERFORMING ORGANIZATION NAME(S) AND ADDRESS(ES) GPS Technologies, Inc., 5095 S. Washington Avenue, Titusville, FL, 32780		8. PERFORMING ORGANIZATION REPORT NUMBER			
9. SPONSORING/MONITORING AGENCY NAME(S) AND ADDRESS(ES)		10. SPONSOR/MONITOR'S ACRONYM(S)			
		11. SPONSOR/MONITOR'S REPORT NUMBER(S)			
12. DISTRIBUTION/AVAILABILITY STATEMENT Approved for public release; distribution unlimited					
13. SUPPLEMENTARY NOTES See also ADM000767. Proceedings of the Twenty-Sixth DoD Explosives Safety Seminar Held in Miami, FL on 16-18 August 1994.					
14. ABSTRACT see report					
15. SUBJECT TERMS					
16. SECURITY CLASSIFICATION OF:			17. LIMITATION OF ABSTRACT Same as Report (SAR)	18. NUMBER OF PAGES 37	19a. NAME OF RESPONSIBLE PERSON
a. REPORT unclassified	b. ABSTRACT unclassified	c. THIS PAGE unclassified			

USAF -45th Space Wing and NASA Headquarters. The program studied the blast wave and fragmentation of bursting gas filled pressure vessels.

The blast wave emanating from a bursting pressure vessel is somewhat similar to that caused by a high explosive detonation. The pressure close in (0 to 10 ft) due to vessel burst is generally lower than high explosive detonation and is a function of burst pressure. Other variations are caused by vessel and failure geometry and distance from a firm reflecting surface.

II. TEST PROGRAM

A test program matrix (Figure 1) was developed that included a series of test plans each with multiple pneumatic vessel bursts. The objective of the program matrix was to force vessel bursts in such a way as to generate worst case blast waves and fragmentation plus bursts that would envelop generally expected vessel failures. Sudden vessel wall disappearance, which is closely approached in a multi-fragment burst, yields a worst case blast wave for a cylindrical vessel. A cylindrical vessel failure which begins as a longitudinal split followed by a circumferential tear is realistic and has been documented.⁶ Endcap failures are also realistic and were studied by Baum.⁷

Eighteen vessels have been burst under pneumatic pressure as shown in Figure 1 and Table 1 and described under "vessels". The TNT equivalence in Table 1 is based on the ideal gas stored energy using isentropic expansion and a conversion factor of 1.545×10^6 ft lb per lb TNT as used by Kinney and Graham.⁸

EQUATIONS

The following equation gives the isentropic energy released by the failure of a vessel containing a volume of ideal gas, V_1 , at a pressure of P_1 . P_2 is the surrounding atmospheric pressure. γ is the specific heat ratio:

$$W = \frac{P_1 V_1}{\gamma - 1} \left[1 - \left(\frac{P_2}{P_1} \right)^{\frac{\gamma - 1}{\gamma}} \right] \quad (\text{eq. 1})$$

Eight high explosive charges were also detonated as part of the test program. These vary in strength from 0.66 lbs pentolite (.9 lbs. TNT equivalence) to 50 lbs composition C-4 (66 lbs TNT equivalence).

The cylindrical vessels were burst along a circumferential line in the vessel center (Test Plans 1 and 2) or at 3/4, 1/4 length or endcap failure (rest Plan #5) or as shown in Figure 1. The

vessels were parallel to the ground and to the 0° - 180° line of the arena as shown in Figure 2. The vessel side wall was placed at the arena center (centerline one foot offset), with the exception of TP #5 and 6A vessels, where the vessels were placed with the vessel centerline coincident with the arena center. All data presented has been corrected for the one-foot offset. The 8.7' and 14' HOB explosive charges were detonated at the center of the arena. The spherical vessels were composite overwrapped pressure vessels (COPV) and were cut with a shaped charge (no groove) around its center. The burst location on the TP #5 vessels varied on the vessels but was always on the arena center. Five pneumatic burst test series, comprising 18 vessels, were conducted at the Naval Surface Warfare Center's (NSWC) Dahlgren, VA explosives test area. This site provides an already wired arena in close proximity to a blockhouse which can prevent penetration of high kinetic energy fragments.

Of the 18 vessels burst using pneumatic pressure (gaseous nitrogen) 16 were cylindrical steel vessels and two were composite spheres. Further information on the vessels is provided in Figure 1 and Table 1. All vessels were 53 cubic feet volume except for the 2.7 cubic feet spheres. The vessel materials and pressure ratings are as follows:

24" cylinders:	SA-372, 2450 psi (ASME Section VIII, Div 1, A.P. 22) (14 were burst)
36" cylinders:	SA-516, 1770 psi (ASME Section VIII, Div. 1) (2 were burst)
spheres:	cryostretched 301 stainless steel liner with Kevlar-epoxy overwrap, 4000 psi (MIL-STD-1522A)

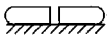


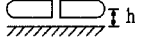
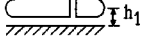


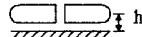
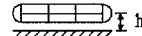
**TABLE 1
PNEUMATIC VESSEL BURSTS**

Vessel #/ Fragment	Vessel Pressure psig	Vessel or Fragment Wt lbs	Fragment Velocity, ¹ FPS	ER ² %	TNT Equivalence lbs
P-2	4700	5775	307	11.6	47.0
P-1	3250	5800	246	11.1	31.7
1-1	1475	5525	145	8.7	13.5
1-3	5425	5825	315	10.6	54.8
1-2	3450	5900	248	10.8	33.8
2-3	3475	5400	265	11.2	34.1
2-2	3450	5300	255	10.3	33.8
1-4	7125	5250	360	9.3	73.4
2-1	3450	5025	250	9.3	33.8
PC ³	3975 ⁴	43.6	982	21.3	2.0
5-1/Lg	3600	3500	245	9.7	35.3
5-1/sm		1425	294		
5-2/lg	3600	3600	242	9.7	35.3
5-2/sm		1500	294		
5-4/lg	3600	4675	218	7.8	35.3
5-4/sm		300	401		
5-3/lg	3600	4675	221	7.9	35.3
5-3/sm		300	398		
6A-1 ⁵	3280	2x800	488	12.0	32.2
6A-2	4000 ⁴	43.6	990	21.3	2.0
6A-3	3300	6100	260	12.9	32.3
6A-4 sidewall	3500	12x362	N/A ⁶	N/A ⁶	34.3
6A-4 endcap		2x352	261		

¹ Average of 2 if only one fragment shown
² ER = Ratio of Kinetic Energy to Isentropic Expansion Energy
³ Preliminary composite overwrapped pressure vessel (COPV)
⁴ Vessel volume = 2.7 cubic feet, all others 53 ft³
⁵ TP #6 Deleted
⁶ Not available, not all fragment velocities evaluated.

TABLE 1 PNEUMATIC VESSEL BURSTS

Figure 1 Test Matrix Showing Actual Bursts

Description	Hydroburst	Prelim. Bursts: S.C. Test Plan	Test Plan #1	Test Plan #2	Test Plan #5* Preliminary TP #4	Test Plan #6A*
Vessel: Material Volumes, ft ³ Diameters, in L/Ds	steel 53 24 11	steel 53 24 11	steel 53 24 11	steel 53 24 11	steel, composite 53, 53, 2.7 24, 22 11, 11, 1	composite, steel 53, 2.7, 53, 53 36, 22, 36, 24 4, 1, 4, 11
Burst Pressure	varies	varies	varies	3500 nominal	varies	varies
Burst Media	water	nitrogen	nitrogen	nitrogen	nitrogen	nitrogen
Number of bursts	1	2	4	3	5	4
Para. Varied	test techniques	pressure (& test techniques)	burst pressure	burst height	split location	vessel, orientation, # of fragments, L/D
Configurations:						 1 @ 36°, P=3280  1 @ 22°: P = 4000  1 @ 36°: P = 3300  1 @ 24°: P = 3500
	#1: P = 7500 no burst #2: P = 6500 burst without shaped charge	#1: P = 4700 no shaped charge #2: P = 3250 with shaped charge, vary groove depth also: shaped charges, with vessels not pressurized	#1: P = 1475 #2: P = 3450 #3: P = 5425 #4: P = 7125	h ₁ = 3.5 h ₂ = 8.7 h ₃ = 14	2 each: P = 3600 1 @ 22°: P = 4000	
Status:	Completed Aug 89	Completed July 90	Completed Jan 91	Completed July 91	Completed June 92	Completed Nov 93
Vessel #s	H1, H2	P2, P1	1-1 through 1-4	2-1 through 2-3	5-1 through 5-4, PC	6A-1 through 6A-4

*TP #3, 4, 6 deleted

FIGURE 1
TEST MATRIX SHOWING ACTUAL BURSTS

FIGURE 2, PRESSURE VESSEL INSTALLED IN NSWC ARENA

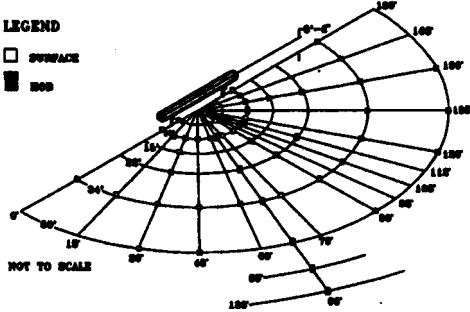


**FIGURE 2, PRESSURE VESSEL
INSTALLED IN NSWC ARENA**

FIGURE 3, TYPICAL VESSEL CROSS SECTION SHOWING GROOVE AND SHAPED CHARGE

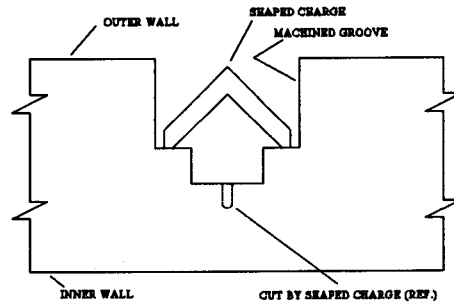


FIGURE 3, TYPICAL VESSEL CROSS SECTION SHOWING GROOVE AND SHAPED CHARGE

Vessel burst was typically initiated by a linear shaped charge (LSC) placed in a pre-machined groove for the steel vessels.

Grooves were circumferentially cut except on vessels 6A-1 and 6A-4 (see Figures 1) which also used longitudinal grooves. The typical vessel groove geometry is shown in Figure 3 with the linear shaped charge and the shaped charge cut area (shown with dotted lines).

BURST INITIATION

Longitudinal stress in the circumferential grooves (for developing axial fragments) ran 40% to 80% of yield strength at completion of pressurization for all vessels except the multi-fragment. The multi-fragment vessels were grooved to have a stress level of approximately 95% of yield stress due to pressurization alone such that following the detonation of the linear shape charge, all groove stresses would exceed the ultimate tensile strength. This was considered necessary to ensure simultaneous separation of all fragments.

There were initial concerns that even a small linear shaped charge (LSC) could bias the blast overpressure measurement. For some vessels (such as vessel P-1 shown in Figure 14) the vessel burst was delayed and the LSC blast pressure has practically returned to ambient prior to the vessel blast shock arrival. For other vessels, the LSC contribution is generally small but is still to be assessed.

TEST HARDWARE

A vessel test stand was designed and fabricated for an initial vessel centerline height of 35 feet. Other heights require replacement of a four inch pipe acting as center post of each stand and guy wire bracing at heights above six feet. At burst the immediate vicinity of the vessel is obscured by dust and a condensation cloud. Several different arrangements of makewire stands, for obtaining close-in velocities, were used during the test program with varying results. The use of the makewire stands was abandoned for the final test series in favor of using the high speed motion pictures alone for obtaining velocity data.

DATA RECORDING

High speed motion picture and video are used for event recording. Approximately 46 channels of fast response piezoelectric pressure transducers are used to record blast overpressure. For the first test, blast transducer ranging was based on the expectation from high explosives of the vessel TNT equivalence⁸. Subsequent ranging is based on test experience and previous work by Bake?.

III. TEST RESULTS

Eighteen vessels have been burst under pneumatic pressure as shown in Table 1 and discussed earlier.

The length to diameter ratios (L/D) shown in the test matrix, Figure 1, are based on length to end of end caps and on the outside diameters. All vessels except 2-2 and 2-3 of TP #2 were burst at a centerline height of 35 feet. All cylinders were burst on a circumferential line near the vessel center except vessels 5-1 through 5-4 of TP#5 and 6A-1 and 6A-4 of TP#6A. The end caps were blown off of vessel 6A-1 and vessel 6A-4 was broken into 14 fragments, three of which were driven to the ground along with a support frame. One spherical composite vessel was split in the horizontal plane in preliminary TP4 (vessel PC) and one was split in the vertical plane in TP 6A (vessel 6A-2).

BLASTWAVE

An explosive blastwave is capable of causing structural damage or causing injuries. The primary measure of the damage potential is the peak intensity, the highest overpressure attained in the rapid pressure rise as the shock passes. The peak overpressure is measured at known distances for comparative purposes. A second measure of destructive capability is the impulse, the area under the positive phase of the overpressure versus time response. Both the overpressure applied to a target and the duration the overpressure is applied affect the target's response.

The peak intensity of the blastwave from a bursting pressure vessel depends on the energy contained in the pressurized gas and on both the vessel geometry and the breakup geometry. The impulse appears to be a function largely of the energy contained in the pressurized gas.

In addition to geometry effects, blast intensity and impulse are compared to TNT equivalence and intensity compared to a computation workbook by Baker, et al⁹. Some pressure versus time wave forms are presented for insight. Burst asymmetry and height of burst effects are also explored.

OVERPRESSURE VERSUS VESSEL PRESSURE

Figure 4 is a plot of peak overpressure at 10 foot and 50 foot ranges versus vessel pressure for 53 cubic feet cylinders burst at mid-length and at a centerline height of 35 feet above ground. Overpressure at 10' and 50' distances for each burst was obtained by a distance regression of log (pressure) versus log (distance) without an angle term, thus asymmetry is averaged out. Regression lines are shown for each distance for convenience in labeling. A reduction in overpressure might be expected at higher vessel pressures due to real gas effects. However arena conditions may cloud this effect in the data collected. The gas flow out of a ruptured vessel near the ground tends to scour the ground, sometimes markedly, particular when the ground is not frozen. This may cause an effect on the data due to attenuation by soft earth or by a change in reflection characteristics. To reduce an effect of the ground condition at the center of the arena, a steel plate of approximately 8' x 8' x 1/4" was used at ground zero for many tests. In contrast none of the high explosive detonations, also at 3.5' height of burst, produced a crater.

FIGURE 4
OVERPRESSURE COMPARISON FROM MID-LENGTH SPLIT

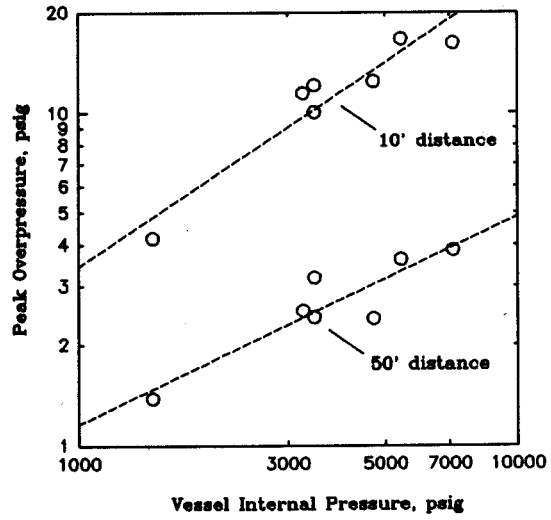


FIGURE 4, OVERPRESSURE COMPARISON
FROM MID-LENGTH SPLIT

BLAST INTENSITY VERSUS GEOMETRY

Figure 5 is a plot of peak overpressure vs. scaled distance for all the vessels burst at a center line height of 35 feet. The open circles are all replotted from Figure 4, of overpressure vs vessel pressure (i.e. coefficients used to compute overpressure at 10' and 50' distances). A regression line is plotted for the open circled points (cylinders burst at mid-length). The two points considerably below the line are for vessel 1-1. No explanation for the low pressures can be offered. The filled points, all at or above the regression line, have a vessel and/or burst geometry which permits a faster venting of the pressurized gas. The open squares and triangles have a burst geometry which increases the exhaust time. All these vessel bursts were described in "Test Results". The scaled distance concept is borrowed from the Sach's or "cube root icing" law for high explosives¹⁰.

The scaled distances were determined by dividing the actual distances by the cube root of the TNT equivalence from Table 1. The data in Figure 5 is from 10' and 50' distances from the regression of log (pressure) vs log (distance) with no angle term for asymmetry.

Also plotted in Figure 5 is an equation showing the overpressure vs scaled distance for the TNT equivalence of the vessel (or for overpressure vs distance for a one pound TNT explosion). It is apparent that increasing the exhaust rate increases the overpressure towards the TNT equivalence line. Some of the points appear to be greater than the TNT equivalence pressure. This can be explained by the fact that the TNT pressures are incident pressures, not amplified by ground reflections, whereas the vessel overpressures are reflected pressures. See "Height of Burst Effects".

FIGURE 5, OVERPRESSURE COMPARISON AT 10', 50' FOR ALL BURSTS

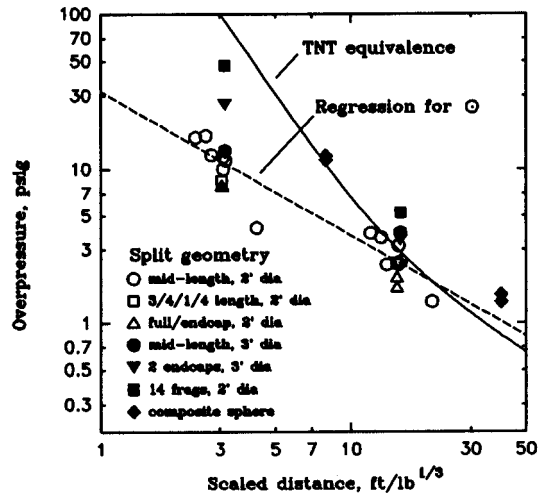


FIGURE 5, OVERPRESSURE COMPARISON AT 10', 50' FOR ALL BURSTS

IMPULSE VERSUS GEOMETRY

Regression coefficients were also obtained for log (impulse) versus log (distance) with no angle term. As before the coefficients were used to compute the impulse at the 10' and 50' range. The distances were then converted to scaled distance by dividing by the TNT equivalence of the vessel energy. The data is plotted in Figure 6 where again a regression line is found for the mid-length split vessels with 2' diameter. The TNT equivalence impulse equation is also plotted. The ordinates are now scaled values as are the abscissas.

The measured impulse values tend to be close to the TNT equivalence for any distance. The fact that some points appear to be greater than TNT equivalence can again be explained by the fact that the TNT equivalence uses incident overpressure and the measured values are reflected.

FIGURE 6, IMPULSE COMPARISON AT 10', 50' FOR ALL BURSTS

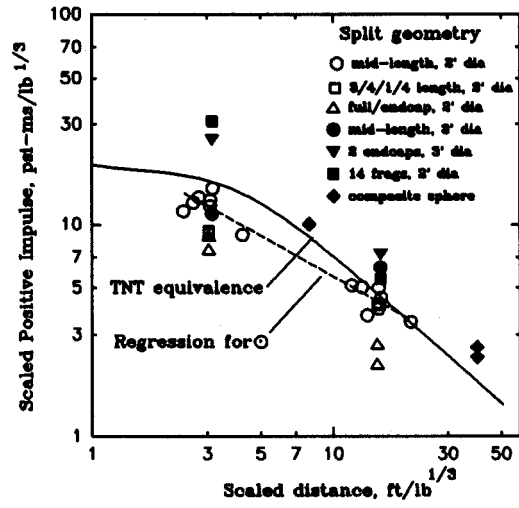


FIGURE 6, IMPULSE COMPARISON AT 10', 50' FOR ALL BURSTS

FIGURE 7, OVERPRESSURE DATA AT 10' AND 34' FOR VESSEL 5-3

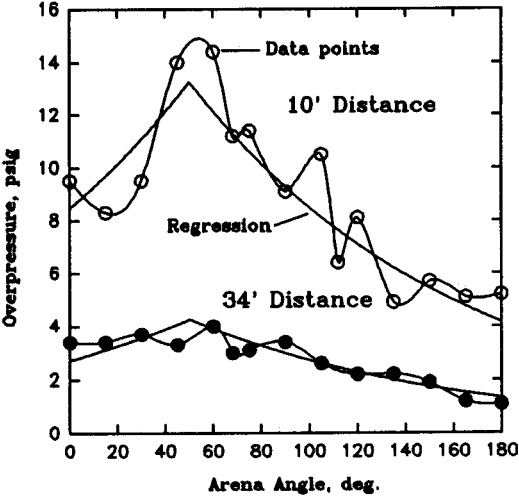


FIGURE 7, OVERPRESSURE DATA AT 10' AND 34' FOR VESSEL 5-3

ASYMMETRY

To look at asymmetry an angle term is added to the regression model, and for "Height of Burst Effects" a term is added which is second order in log (distance), yielding:

$$\log_e P = B_1 + B_1 \log_e D + B_3 A + B_4 (\log_e D)^2 \quad (\text{eq.2})$$

where: P = pressure, psig (or I= impulse, psi-ms)
D = distance (slant height except for height of burst measurements) from vessel center (and burst point)
A = absolute value of angle from reference blast angle (reference angle found by selecting one of 20 overpressure curve fits, 00 to 1000 using 50 increments, having least sum square errors)
B₁ = coefficients, B₄ is zero unless 2nd order provides an accuracy improvement (vessels 2-1 through 2-3 only)

The high explosive detonation and the spherical composite vessel, vessel PC, were quite symmetrical. The vessels of Test Plan S were the least symmetrical particularly the endcap vessels. Overpressure data for the 10 ft. and 34 ft. distances for endcap vessel 5-3 are shown in Figure 7. One third of the total data was recorded at each distance. Data points are connected with a cubic spline for clarity. The regression lines fit the overpressure data, Figure 7, reasonably well at both 10 ft. and 34 ft. distances. The regression fit to the impulse data, Figure 8, is poor because of the data scatter at 10 ft. distance and because the same reference angle (equation 2, definitions) was used as for overpressure. Both endcap vessels showed very similar overpressure and impulse distribution. The best fit reference angle (and strongest blast angle) varied from 50° for vessel 5-3, shown, to 45° for vessel 5-4.

FIGURE 8, IMPULSE DATA AT 10' AND 34' FROM VESSEL 5-3

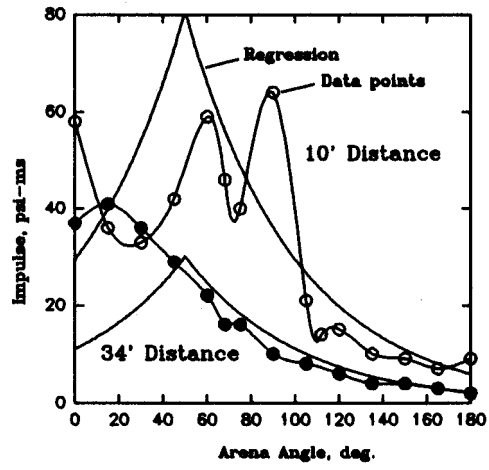


**FIGURE 8, IMPULSE DATA AT
10' AND 34' FROM VESSEL 5-3**

FIGURE 9, 14' HOB PRESSURE VESSEL

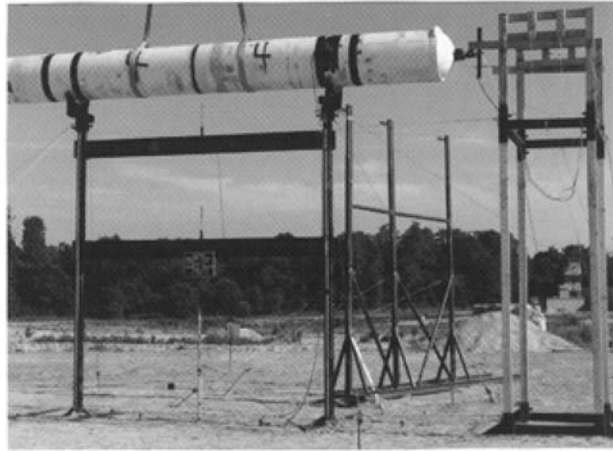


FIGURE 9, 14' HOB PRESSURE VESSEL

HEIGHT OF BURST EFFECTS

The reflection of the shock front at a surface, such as the ground, intensifies the peak overpressure from the blast. This effect is well documented in the literature for explosives-. Height of burst detonations were made using 45# pentolite at 35, 8.7 and 14.0 ft HOB and 3450 psi (nominal) pressure cylindrical steel vessels at the same height. The high explosive was chosen to yield approximately the same overpressure as the vessels at 10 foot distance so that all measurements are within recorder range without re-scaling.

The difference between the incident (or non-reflected pressure) and the reflected pressure wave cannot always be clearly discerned at a reflected (i.e. ground) transducer location. Accordingly, pressure measurements were made above ground under the vessel when burst at 8.7 ft and 14 ft HOB and at vessel height at 10, 15 and 22 foot distances along the ground. Figure 9 shows the setup for the 14 ft HOB vessel test. These measurements are used for the incident pressure for comparison to ground measured pressures. (Incident pressures for the pentolite blast were measured only on the auxiliary HOB transducer stand shown in Figure 9). Compared to reflected data the incident pressure equations are therefore based on less data and closer in measurements and at straight line distances (as opposed to a slant height) with only the ground distance being considered.

Figure 10 shows reflection factors for the three high explosives tested and Figure 11 shows the reflection factors for three pressure vessels tested. Second order (log-log) curve fits were used for HOB data reduction where they yielded better fits. Reflection factors are all based on the maximum pressure array for mid-length split vessels. Comparing the two figures shows that reflection factors were obtained for pressure vessel blast waves, similar to high explosive, but of a lesser magnitude and dissimilar appearance. A minimum reflection factor of 2 is expected but did not occur with the center split cylinders.

FIGURE 10
MEASURED REFLECTION FACTORS FOR HIGH EXPLOSIVE

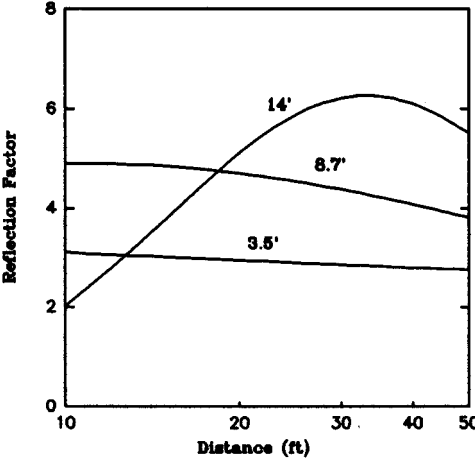
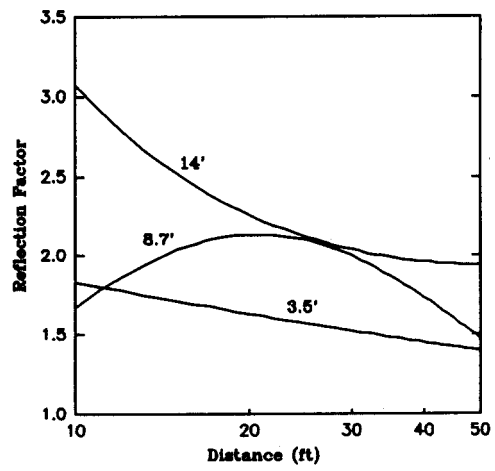


FIGURE 10, MEASURED REFLECTION FACTORS FOR HIGH EXPLOSIVE

**FIGURE 11, REFLECTION FACTORS
FOR VESSEL BURST**



**FIGURE 11, REFLECTION FACTORS
FOR VESSEL BURST**

OVERPRESSURE RESULTS VERSUS THEORY

The incident shock overpressure at the vessel surface, P_s , may be calculated using the one dimensional shock tube equation which may be found in references 9 and 11. Conditions for the lowest pressure burst (1475 psig, 31°F ambient temperature and 65°F gas temperature) yield a P_{s0} of 82.9 psig. Conditions for the highest pressure burst (7125 psig, 93°F ambient temperature and 124° gas temperature) yield a P_{s0} of 133.2 psig.

Baker⁹ uses P_{s0} as a starting point in calculating the overpressure due to a bursting pressure vessel. Baker's curves (based on one-dimensional hydrocode calculations), assume sudden vessel wall disappearance, hence the theoretical predictions are typically higher than can be achieved in a real vessel burst since a finite time is required for the gas to flow to the rupture and then exhaust. Two plots are provided to demonstrate the comparison of results versus theory. In both cases the vessel venting is rapid enough to approach the disappearing wall assumption.

Figure 12 presents data for the initial composite sphere burst, vessel PC. The measured data was recorded at ground level and hence is reflected data. The calculated line using "volume correction" uses a volume of twice actual as a partial reflection correction. This increases the pressure at the closest point by 26%. The curve having additional ground corrections includes a factor of 2 times the "volume" curve at near field and 1.1 at far field. (Calculated data procedure includes picking points from curves of normalized values, hence the lack of smooth curves.)

Figure 13 is the burst of the multi-fragment vessel, burst 6A-4. Figure 14 presents data for cylinder burst 6A-4. This cylinder broke into 14 fragments of approximately equal weight, which also approximates the disappearing wall assumption. The figure presents curves for measured, calculated with volume correction and a curve which contains both cylinder correction factors and ground reflection factors. The cylinder correction factors (which Baker et al stated are "very crude") varied from 4.5 in the near field to 1.4 in the far field. The reflection correction factors varied from 2.0 in the near field to 1.1 in the far field.

FIGURE 12, COMPARISON OF COMPOSITE SPHERE OVERPRESSURES

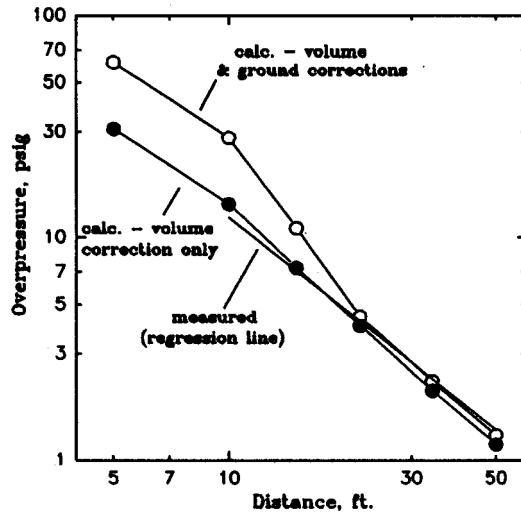


FIGURE 12, COMPARISON OF COMPOSITE SPHERE OVERPRESSURES

FIGURE 13, BURST OF MULTI-FRAGMENT VESSEL



**FIGURE 13, BURST OF
MULTI-FRAGMENT VESSEL**

FIGURE 14
COMPARISON OF MULTI-FRAGMENT CYLINDER
OVERPRESSURES

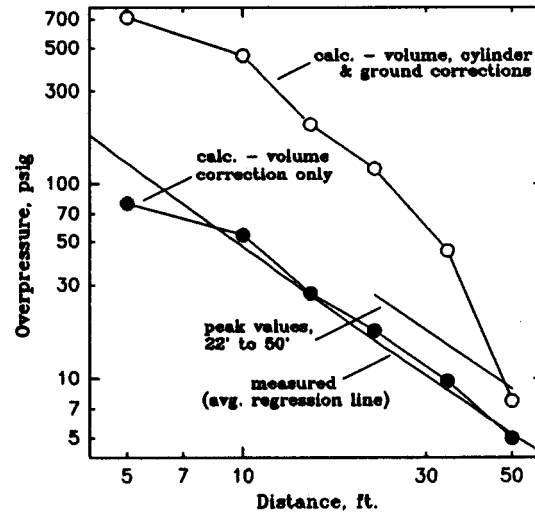


FIGURE 14, COMPARISON OF MULTI-FRAGMENT CYLINDER OVERPRESSURES

It is doubtful that much greater overpressures from these two vessels would ever occur accidentally since this would require a greater number of fragments with attendant faster venting. The corrections to the cylinder calculations which are required by the reference appear to be excessive except at the 50 ft. distance.

PRESSURE VERSUS TIME WAVEFORM

Ideal high explosive waveform characteristics include a sharp rise followed by an exponential decay. Two of the traces in Figure 15 are similar to high explosive response. All recordings shown were made from transducers located in the same general location: at a range of 10 feet to 15 feet and within 300 of normal to the long vessel axis.

Figure 15 presents data from vessel bursts P-1, 6A-2 and 6A-4. P-1 is a cylinder burst about its mid-length. The square wave was seen at distances of 22 feet and closer. At greater distances the waveform transitioned to an exponential decay. The pre-burst pressure rise is the LSC detonation. Vessel 6A-2 is the latter composite sphere. The equatorial split presented a large ratio of exhaust area to vessel volume compared to the cylinder. Additionally the lightweight fragments accelerate rapidly and minimally reduce the vent area at the beginning of launch. The sphere waveform has the sharp peak, semi-exponential and second shock similar to a high explosive blast. Vessel 6A-4 was burst into 14 fragments, providing a large

vent area for a cylindrical burst. The waveform has a sharp peak, a generally, although somewhat ragged, exponential decay and second shock. The overpressure measured was greater than with any other cylindrical burst.

FIGURE 15, VESSEL BURST OVERPRESSURE TIME RESPONSE

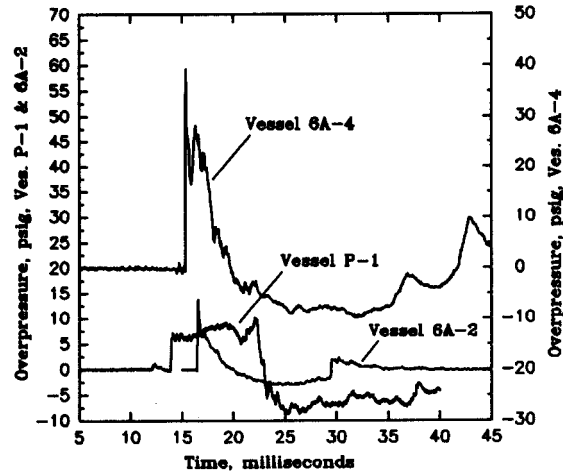


**FIGURE 15, VESSEL BURST OVERPRESSURE
TIME RESPONSE**

FRAGMENTATION

Like the explosive blastwave, fragmentation is also capable of causing structural damage or causing injuries. However, fragmentation presents a much different problem for the designer. While the damage potential from the blastwave is a function of distance from the failure and decreases rapidly with distance, fragmentation is capable of causing damage at great distances. In this test program significant damage occurred to a number of trees at distances exceeding 1000 ft. The problem facing the designer is to predict the fragment size, trajectory, and velocity. In this section the fragment velocity is explored by comparing the measured velocities to predicted velocities based on previous work by Baum¹² and a computer model developed by ACTA¹³.

FRAGMENT TYPE AND RANGE

With the exception of the multi-fragment vessel included in test plan #6A, all of the vessels were split into two main fragments. The fragments from the cylindrical steel vessels varied in size from end caps weighing 300 lbs to the full vessel length weighing 4675 lb. Table 2 includes vessel and fragment numbers, burst pressure, vessel or fragment weight and the total distance traveled for fragments for two selected test series. In general, the west fragment traveled a greater distance than the east fragment due to the connection of the pressurization tubing to the east end of the vessel and the greater number of obstructions east of the arena.

FRAGMENT VELOCITY VERSUS GEOMETRY

In comparing the measured fragment velocity to previous work by Baum it was necessary to classify the fragments into the missile geometries proposed by Baum. The classifications used include: cylindrical vessel end cap missile, cylindrical vessel rocket missile, fragments generated by disintegration of a cylindrical vessel, and fragments generated by disintegration of a spherical vessel. The fragments from the COPV were classified as fragments generated by the disintegration of a spherical vessel in lieu of hemispherical fragments since the work by Baum did not include a Recommend Upper Limit Velocity for a hemispherical fragment resulting from a gas burst. Furthermore, the COPV burst was observed to have multiple fragments (especially along the split line) even though the failure was initiated by a circumferential cut.

FIGURE 16, COMPARISON OF FRAGMENTS

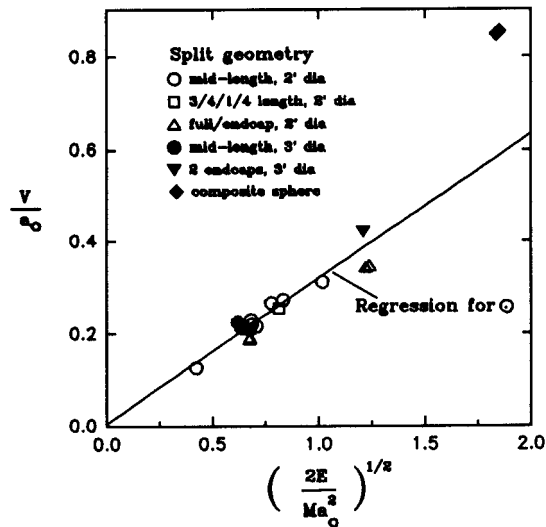


FIGURE 16, COMPARISON OF FRAGMENTS

Figure 16 is a plot of fragment velocity expressed as a fraction of the velocity of sound versus energy/mass ratio for the fragments from all vessels as in Baum¹². In this figure, E is the expansion energy (we substituted W from equation 1) and M is the mass. In Figure 16 the ratio of fragment to sonic velocity is plotted against a function of fragment size and acceleration for rocket type missiles as defined by Baum¹⁴ and provided in expression 1. Baum's recommended upper limit velocity is also provided.

EQUATION

$$F \left(\frac{L}{R}\right)^{\frac{1}{2}} \quad (\text{exp. 1})$$

where:

$$F = \frac{P_o AR}{Ma_o^2}$$

(dimensionless initial acceleration)

- L = Vessel length
- R = Vessel radius
- P_o = Rupture pressure
- A = Projected area of fragment
- M = Mass of fragment
- a_o = Velocity of sound

Table 3 presents the data for the other fragment classifications and compares them to the correspond~g Baum Recommended Upper Limit Velocity. As seen in the Figure 17 and Table

3 the actual fragment velocities were approximately 50% to 70% of Baum's Recommended Upper Limit Velocity for all of the heavy steel fragments. In Baum's work, he reported data which more closely approached the Recommended Upper Limit Velocity. One noted difference in work by Baum and the tests conducted in this program is that much of the vessel data used by Baum came from smaller, lighter weight vessels and fragments. However in comparing Burst Study data to Baum's limit velocities it was found that the limits were consistently useable albeit conservative.

**TABLE 2
FRAGMENT DISTANCES**

Vessel #/ Fragment	Vessel Pressure, psig	Vessel or Fragment Wt, lbs	Distance Recovered, feet	Comments
1-1	1475	5525	409E 404W	
1-2	3450	5900	not recorded	
1-3	5425	5825	783E 1347W	West fragment cut tree at 40' height on final bounce (1327')
1-4	7125	5250	1027E, 1271W	West fragment broke off 10 trees with diameters between 4" & 12"
6A-1	3280	2x800	1644E, 1176W	East fragment was ballistic last 757' (bounced off camera shelter)
6A-2	4000	43.6	390W, 213E	overwrap = 243W, 186E
6A-3	3300	6100	1156E, 1176W	
6A-4 sidewall	3500	12x362	10 to 1640 (563 avg)	3 pieces driven down and bounced, average of others = 740'
6A-4 endcap		2x352	194E, 1643W	East endcap struck dirt mound

TABLE 2 FRAGMENT DISTANCES

**TABLE 3
MISCELLANEOUS FRAGMENT VELOCITIES VERSUS BAUM'S LIMIT VELOCITIES**

Vessel #	Pressure psig	Fragment- number	Weight each, lbs	Average Fragment Velocity/a₀	Upper Limit Velocity/a₀
5-3	3600	Endcap-1	300	0.343	.647
5-4	3600	Endcap-1	300	0.346	.647
6A-1	3280	Endcap-2	800	0.421	.666
6A-4	3500	Endcap-2	352	0.226	.589
6A-4	3500	Sidewall-12	362	N/A*	.415
PC	3975	Hemisphere-2	21.8	0.847	1.002
6A-2	4000	Hemisphere-2	21.8	0.854	1.005
*Not yet available, some sidewall fragment velocities not yet determined.					

**TABLE 3 MISCELLANEOUS FRAGMENT VELOCITIES VERSUS
BAUM'S LIMIT VELOCITIES**

FIGURE 17, ROCKET TYPE FRAGMENT COMPARISON

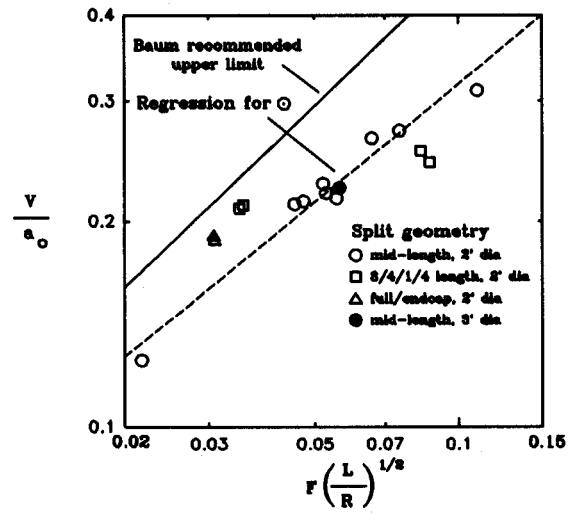


FIGURE 17, ROCKET TYPE FRAGMENT COMPARISON

FIGURE 18, CALCULATED AND MEASURED FRAGMENT VELOCITIES FOR CYLINDRICAL VESSELS

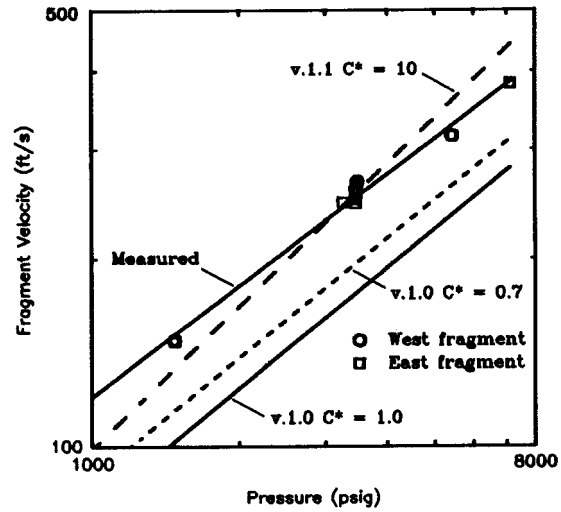


FIGURE 18, CALCULATED AND MEASURED FRAGMENT VELOCITIES FOR CYLINDRICAL VESSELS

CALCULATED FRAGMENT VELOCITIES

A fragment velocity program¹³, based upon a work by Taylor and Price¹⁵ will be modified to the extent practicable in an effort to closely compute the measured velocities in Table 1. Table 1 shows fragment velocities and energy ratio (ER) for all the pneumatic burst vessels. The energy ratio is defined herein as the ratio of the kinetic energy of the two (or more) fragments to the total stored energy of the gas using isentropic expansion of an ideal gas to atmospheric pressure. This ratio ran around 9% for the heavy steel cylindrical vessel fragments to about 21% for the light spherical composite vessel (COPV) fragments which attained a high velocity.

Figure 18 is a plot of fragment velocity versus pressure for mid-length split steel vessels of Table 1, all of which were of the same design. The average fragment velocity is shown in Table 1 (where both velocities could be obtained), whereas Figure 18 shows separate velocities for the east and west fragments.

Figure 18 also shows lines of velocity versus vessel pressure from computer calculations. Shown are lines calculated using the original model (ACTA, Inc. code version 1.0) and discharge coefficients, k , of 0.7 and 1.0. A discharge coefficient of 0.6 to 1.0 is expected from orifice flow theory. It was found² that discharge coefficients of .41 to .55 were required to match measured fragment velocities for tested configurations. The program was revised (code version 1.1) to limit the flow area to the actual exhaust area. A line of velocities is also shown in Figure 18 using the revised program and a discharge coefficient of 1.0. This changed the slope of the line and indicates that more work is required on the program.

Other vessel burst computations to be assessed include very lightweight fragments such as vessels PC and 6A-2 and variation in burst length such as in vessel 5-1 through 5-4.

The program computes supersonic fragment velocities for the light weight fragments. Baum¹⁴ indicates a possibility of supersonic fragments and Pittman¹⁶ measured supersonic velocities, but we have not.

FUTURE EFFORTS

Future (as of November 93) efforts include a test report on TP 6A testing, a technical report covering all Burst Study efforts and a workbook to assist safety engineers in assessments. The workbook will include the work of other authors.

SUMMARY & CONCLUSIONS

Substantial documentation exists for estimating injury and damage from blast wave overpressure and impulse and from fragment impact velocity and mass. However much of the data compares a pressure vessel burst to a high energy explosive blast. Additional vessel burst testing has been accomplished to augment existing data in quantifying pressure vessel burst characteristics. The current test program provides a mix of vessel failure modes, pressures,

and other variables. This data, together with data from other researchers will permit assessing the results of different assumed options for vessel failures such that the installation designer or user can weigh the likelihood of such failures and the hazards should they occur.

This paper is the final progress report on the pressure vessel burst test program. Pneumatic burst testing has been accomplished and data analysis on latter tests is in progress. Further analysis will clarify results and provide conclusions to be presented in the future.

Partial conclusions are as follows:

1. Comparison of overpressure vs. distance for pressure vessels with I~I equivalence overpressures is complicated by ground reflection factors. Reflection factors are not necessarily constant although they are sometimes treated as a constant factor of 2 times incident overpressure. Published values of overpressure for iii are incident pressures. Vessel burst overpressure decrease at a less rapid rate with distance than TNT.
2. Vent area and vent rate from a pressure vessel have a large effect on overpressure.
3. Average impulse appears to be the same as the TNT equivalent, particularly for a fast exhaust vessel (larger diameter for given volume) and failure (multiple fragments) geometry.
4. Pressure vessel overpressure reflection factors appear to be less than half that of a high explosive blast having a similar overpressure at a 10 foot range and may be less than two for certain heights and burst geometries.
5. Additional effort is required for computer calculation of accurate fragment velocities.
6. Correction factors for calculating overpressures using NASA CR-134906 appear to be excessive, especially cylinder correction factors which may be four times actual results.
7. Additional height of burst testing should be conducted, particularly for rapid venting vessel/burst geometries.
8. Burst Study data provides concurrence that Baum's applicable upper limit velocities are useful if somewhat conservative.

REFERENCES

- ¹Cain, Sharp, Coleman, "Pressure Vessel Burst Test Program: Initial Program Paper," AIAA 90-2348, July 1990.
- ²Cain, Sharp, Coleman, "Pressure Vessel Burst Test Program Progress Paper No. 2", AIAA 91-2091, June 1991.
- ³Cain, Sharp, Coleman, "Pressure Vessel Burst Test Program Progress Paper No. 3", AIAA 92-3608, July 1992.
- ⁴Cain, Sharp, "Pressure Vessel Burst Test Program Progress Paper No. 4", AIAA ~2100, June 1993.
- ⁵Coleman, M. et al, "A Review of Energy Release Processes From the Failure of Pneumatic Pressure Vessels," ESMC-Th-88-03, Eastern Space and Missile Center, August 1988, pages 7, 32, 35, 38, 40, 53.
- ⁶Murray, Assessment of a Pressure Vessel Removed from LC-17 for Destructive Testing, National Aeronautics and Space Administration (NASA) Kennedy Space Center, Dec 1986.
- ⁷Baum, Rupture of a Gas Pressurized Cylindrical Pressure Vessel. The Dynamics of End-Cap Missiles, Institute of Chemical Engineers, vol. 67, July 1989.
- ⁸Kinney and Graham, Explosive Shocks in Air 2nd ed, Springer Verlag, 1985.
- ⁹Baker, W. et al, "Workbook for Predicting Pressure Wave and Fragment Effects of Exploding Propellant Tanks and Gas Storage Vessels", NASA CR-134906, November, 1975.
- ¹⁰ASME/ANSI, Estimating Airblast Characteristics for Single Point Explosions in Air, With a Guide to Evaluation of Atmospheric Propagation and Effects, ANSI S2.20, 1983.
- ¹¹Leipman and Roshko, "Elements of Gas Dynamics", Wiley, 1977, pages 80, 81.
- ¹²Baum, "The Velocity of Missiles Generated by the Disintegration of Gas-Pressurized Vessels and Pipes", American Society of Mechanical Engineers Journal of Pressure Vessel Technology November 1984.
- ¹³Program ADABATIC_BURST_CYLINDER, unpublished software, ACTA Inc., Oct. 91.
- ¹⁴Baum, "Disruptive Failure of Pressure Vessels: Preliminary Design Guidelines for Fragment Velocity and the Extent of the Hazard Zone", Transaction of the ASME Journal of Pressure Vessel Technology. May, 1988.

¹⁵Taylor, T.D. and Price, C.S., "Velocities of Fragments from Bursting Gas Reservoirs", Journal of Engineering for Industry, November, 1971.

¹⁶Pittman, "Blast and Fragment Hazards from Bursting High Pressure Tanks", Naval Ordnance Laboratory, May, 1972.

ACKNOWLEDGMENTS

The program described is ongoing under the direction of the USAF -45th Space Wing and is jointly directed and supported by NASA Headquarters. The program is performed by the Pressure Systems Technology Department of GPS Technologies and involves the effort of other government centers, subcontractors and suppliers. We would like to thank all for the support and input to the program, especially Mr. Lou Ullian and Mr. Bobby Webb of 45SPW and Mr. Wayne Frazier of NASA Headquarters. We would also like to thank Mr. Kent Rye of the Naval Surface Warfare Center for his efforts and Ms. Theresa Cooper of GPS Technologies for typing and graphics support.